Switching Between OSTBC and Spatial Multiplexing with Linear Receivers in Spatially Correlated MIMO Channels

Antonio Forenza[†], Matthew R. McKay[‡*], Iain B. Collings[*], and Robert W. Heath, Jr.[†]

[†]Wireless Networking and Communications Group (WNCG), ECE Department, The University of Texas at Austin, TX, USA
{forenza, rheath}@ece.utexas.edu

[‡]Telecommunications Lab., Sch. of Elec. and Info Engineering, University of Sydney, Australia, mckay@ee.usyd.edu.au

[*]Wireless Tech. Lab., ICT Centre, CSIRO, Australia, Iain.Collings@csiro.au

***Abstract*— We present a low complexity adaptive transmission approach for spatially correlated MIMO channels. The proposed scheme adaptively switches between orthogonal space-time block codes (OSTBC) and spatial multiplexing (SM), depending of the channel correlation and SNR. We derive an exact closed-form expression and tight upper bound on the OSTBC capacity in double-correlated channels, and examine the relative capacity of OSTBC and SM in terms of the spatial correlation. We then derive efficient closed-form BER expressions for practical OSTBC transmission employing bit-interleaved coded modulation (BICM). Based on these results, we propose a practical adaptive algorithm which selects the combination of MIMO transmission scheme (OSTBC or SM), and BICM mode, which achieves the highest spectral efficiency whilst satisfying a pre-defined BER.** [1]

I. Introduction

Multiple-input multiple-output (MIMO) technology exploits the spatial components of the wireless channel to improve capacity and bit error rate (BER) performance of communication systems, through diversity or multiplexing transmission techniques. Diversity schemes, such as orthogonal space-time block codes (OSTBC) [1], are conceived to combat channel fading, providing increased link robustness. Spatial multiplexing (SM) enables transmission of multiple parallel data streams as a means to enhance systems throughput [2]. These benefits can be simultaneously achieved in MIMO systems, according to the theoretical diversity/multiplexing tradeoffs derived in [3]. One practical implementation is to adaptively switch between diversity and multiplexing transmission schemes, by tracking the changing channel conditions.

A number of adaptive MIMO transmission techniques have been proposed thus far. The diversity/multiplexing switching method in [4] was designed to improve BER for fixed rate transmission, based on instantaneous channel quality information. Alternatively, statistical channel information can be employed to enable adaptation as in [5], resulting in reduced feedback overhead and number of control messages. The adaptive transmission algorithm in [5] was designed to enhance spectral efficiency for predefined target error rate, based on channel time/frequency selectivity indicators. In [6, 7] we proposed similar low-feedback adaptive approaches, exploiting the channel *spatial selectivity* to switch between beamforming and spatial multiplexing.

[1]The work of A. Forenza and R. W. Heath, Jr. is supported by Freescale Semiconductor, Inc., the National Science Foundation under grant number CCF-514194 and the Office of Naval Research under grant number N00014-05-1-0169.

In this paper we examine adaptive schemes which require even less feedback than [6, 7], by adapting between the open-loop MIMO schemes OSTBC and SM, with low-complexity linear receivers. We first derive new closed-form expressions for the ergodic capacity of OSTBC in spatially-correlated Rayleigh MIMO channels, and then find theoretical tradeoffs between OSTBC and SM based on capacity crossing points. We then compute efficient closed-form BER expressions for OSTBC with bit-interleaved coded modulation (BICM), based on a saddlepoint approximation originally proposed in [8] for the single-input single-output (SISO). Finally, we propose a practical adaptive algorithm, based on the derived BER expressions, and show significant improvements in BER and spectral efficiency over non-adaptive systems. Given the low-complexity MIMO transceivers, the low feedback overhead required for adaptation, and the relevant performance gains, the proposed method provides an attractive solution for future generation MIMO systems, particularly in the context of the standards IEEE 802.11n, IEEE 802.16e and 3GPP LTE.

II. System and Channel Models

Consider a narrowband MIMO system with N_t transmit and N_r receive antennas, modeled for each channel use by

$$\mathbf{r} = \sqrt{\frac{E_s}{N_t}}\,\mathbf{H}\mathbf{a} + \mathbf{n} \tag{1}$$

where $\mathbf{r} \in \mathbb{C}^{N_r \times 1}$ is the receive signal vector, $\mathbf{a} \in \mathbb{C}^{N_t \times 1}$ is the transmit signal vector subject to the power constraint $\mathcal{E}\{||\mathbf{a}||_2^2\} = N_t$, $\mathbf{n} \in \mathbb{C}^{N_r \times 1}$ is the additive white Gaussian noise (AWGN) vector with covariance matrix $\mathcal{E}\{\mathbf{n}\mathbf{n}^\dagger\} = N_o\mathbf{I}_{N_r}$, and $\mathbf{H} \in \mathbb{C}^{N_r \times N_t}$ is the MIMO channel matrix. The SNR is defined as $\gamma = E_s/N_o$.

We model the spatially-correlated Rayleigh MIMO channel as[2]

$$\mathbf{H} = \mathbf{R}^{1/2}\mathbf{Z}\mathbf{S}^{1/2} \tag{2}$$

where $\mathbf{Z} \in \mathbb{C}^{N_r \times N_t}$ contains independent entries $\sim \mathcal{CN}(0,1)$, and $\mathbf{S}$ and $\mathbf{R}$ denote the transmit and receive spatial correlation matrices, respectively. We normalize the MIMO channel matrix such that $\mathcal{E}\left[||\mathbf{H}||_F^2\right] = N_r N_t$ and define $\mathbf{Q} = \mathbf{S} \otimes \mathbf{R}$. The matrices $\mathbf{Q}$, $\mathbf{S}$ and $\mathbf{R}$ have the eigenvalue decompositions

$$\mathbf{Q} = \mathbf{U}_q\mathbf{\Lambda}_q\mathbf{U}_q^\dagger, \qquad \mathbf{S} = \mathbf{U}_s\mathbf{\Lambda}_s\mathbf{U}_s^\dagger, \qquad \mathbf{R} = \mathbf{U}_r\mathbf{\Lambda}_r\mathbf{U}_r^\dagger. \tag{3}$$

[2]We use $(\cdot)^*$ to denote conjugation, $(\cdot)^T$ to denote transposition, $(\cdot)^\dagger$ to denote conjugation and transposition, $|\cdot|$ to denote the absolute value or determinant of a matrix, $||\cdot||_F$ to denote the Frobenius norm.

0-7803-9392-9/06/$20.00 (c) 2006 IEEE

To verify the analytical results presented in this paper, we consider the exponential correlation model at the transmitter and receiver $\mathbf{R}_{i,j} = \rho_{\text{rx}}^{|i-j|}$ and $\mathbf{S}_{i,j} = \rho_{\text{tx}}^{|i-j|}$, where ρ_{rx} and ρ_{tx} are the receive and transmit spatial correlation coefficients between adjacent antennas. To make our discussion concrete, we also evaluate the performance of the proposed adaptive algorithm in realistic propagation environments simulated through the COST-259 physical channel model [9].

For OSTBC transmission with a maximum-ratio combining (MRC) receiver, we have the following equivalent input-output extension to (1) as in [10]

$$\mathbf{z} = \sqrt{\gamma}\|\mathbf{H}\|_F^2\mathbf{a} + \underline{\mathbf{n}} \tag{4}$$

where $\underline{\mathbf{n}} \sim \mathcal{CN}\left(\mathbf{0}_{n_s\times 1}, \|\mathbf{H}\|_F^2\mathbf{I}_{n_s}\right)$.

III. Comparison of OSTBC and SM Capacity in Spatially-Correlated Channels

A. Capacity of OSTBC in Double-Sided Correlated Channels

In this section we derive a new closed-form expression and a much simpler upper bound expression for the capacity of OSTBC with a MRC receiver in spatially-correlated channels. These results will be used to investigate the relative performance of OSTBC with respect to SM transmission in various correlated channel scenarios.

The ergodic capacity of OSTBC can be expressed as

$$C_{\text{OSTBC}} = R_{\text{c}}\mathcal{E}\left[\log_2\left(1 + \frac{\gamma}{R_{\text{c}}N_t}\|\mathbf{H}\|_{\text{F}}^2\right)\right] \tag{5}$$

where $R_{\text{c}} = n_s/N$ is the rate of the OSTBC, n_s is the number of symbols transmitted per block and N is the number of symbol periods per block. For double-sided spatially correlated channels we find

$$\begin{aligned}\|\mathbf{H}\|_{\text{F}}^2 &= \text{vec}(\mathbf{H})^{\dagger}\text{vec}(\mathbf{H}) \\ &= \text{vec}(\mathbf{Z})^{\dagger}\mathbf{\Lambda}_q\text{vec}(\mathbf{Z}) \\ &= \frac{1}{2}\sum_{i=1}^{r}\lambda_{q,i}\varepsilon_i\end{aligned} \tag{6}$$

where $r = \text{rank}(\mathbf{Q})$, $\lambda_{q,i}$ are the non-zero diagonal entries of $\mathbf{\Lambda}_q$ in (3) and ε_i's are i.i.d. exponentially distributed random variables. Note that we invoke the property

$$\text{vec}(\mathbf{H}) = (\mathbf{S}^{1/2}\otimes\mathbf{R}^{1/2})\text{vec}(\mathbf{Z}) = \mathbf{Q}^{1/2}\text{vec}(\mathbf{Z}) \tag{7}$$

following from (2). We now define $\eta = \sum_{i=1}^{r}\lambda_{q,i}\varepsilon_i$, which is clearly a central quadratic form in Gaussian random vectors. Using a general result from [11], the p.d.f. of η is found to be

$$f(\eta) = \sum_{i=1}^{r}\left(\prod_{j=1,j\neq i}^{r}\frac{\lambda_{q,i}}{\lambda_{q,i}-\lambda_{q,j}}\right)\frac{\exp\left(-\frac{\eta}{2\lambda_{q,i}}\right)}{2\lambda_{q,i}}. \tag{8}$$

Using (5) and (8), the capacity is now given by

$$\begin{aligned}C_{\text{OSTBC}} = R_{\text{c}}&\sum_{i=1}^{r}\prod_{j=1,j\neq i}^{r}\left(\frac{\lambda_{q,i}}{\lambda_{q,i}-\lambda_{q,j}}\right) \\ &\times\int_0^{\infty}\log_2\left(1+\frac{\gamma}{2R_{\text{c}}N_t}\eta\right)\frac{\exp\left(-\frac{\eta}{2\lambda_{q,i}}\right)}{2\lambda_{q,i}}\text{d}\eta.\end{aligned} \tag{9}$$

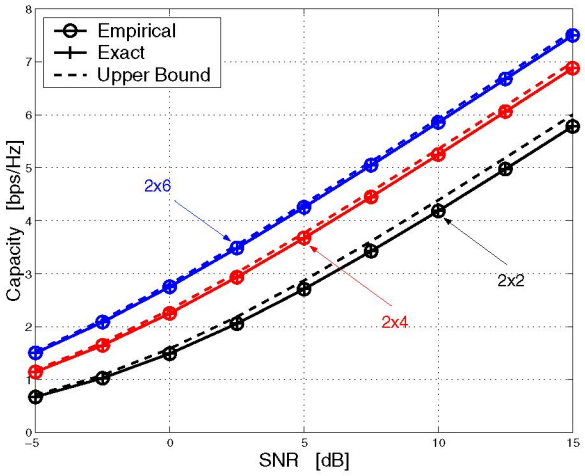

Fig. 1. Empirical, exact and upper bound to the ergodic capacity of OSTBC for 2x2, 2x4 and 2x6 MIMO systems. The exponential model is used, with $\rho_{\text{tx}} = 0.5$ and $\rho_{\text{rx}} = 0.1$.

To evaluate the integrals in (9) we use the property [12]

$$\int_0^{\infty}\ln(1+\beta x)\exp(-\mu x)\,\text{d}x = -\frac{1}{\mu}\exp\left(\frac{\mu}{\beta}\right)\text{Ei}\left(-\frac{\mu}{\beta}\right) \tag{10}$$

for $\text{Re}(\mu) > 0$ and $-\pi < \arg\beta < \pi$, where $\text{Ei}(\cdot)$ is the exponential integral. For Hermitian positive definite $\mathbf{Q}$, the required conditions are met, and we use (10) to obtain

$$\begin{aligned}C_{\text{OSTBC}} = -\frac{R_{\text{c}}}{\ln 2}\sum_{i=1}^{r}\Bigg(&\prod_{j=1,j\neq i}^{r}\left(\frac{\lambda_{q,i}}{\lambda_{q,i}-\lambda_{q,j}}\right) \\ &\times\exp\left(\frac{R_{\text{c}}N_t}{\gamma\lambda_{q,i}}\right)\text{Ei}\left(-\frac{R_{\text{c}}N_t}{\gamma\lambda_{q,i}}\right)\Bigg).\end{aligned} \tag{11}$$

We clearly see that the OSTBC capacity depends explicitly on the long-term channel characteristics through the eigenvalues of the spatial correlation matrices.

We can derive a simpler expression which provides more insights by examining the upper bound on OSTBC capacity by applying Jensen's inequality to (5) to obtain

$$C_{\text{OSTBC}} \leq R_{\text{c}}\log_2\left(1+\frac{\gamma}{R_{\text{c}}}N_r\right). \tag{12}$$

Note that this upper bound applies for both single-sided and double-sided correlated Rayleigh MIMO channels.

In Fig. 1 we compare the capacity expression (11) and upper bound (12) with empirically generated (simulated) capacity curves, in exponentially correlated channels with various antenna configurations. We see that the closed-form expression (11) is exact and the upper bound (12) is tight in all cases.

B. Relative Capacity Investigation of OSTBC and SM

An upper bound to the ergodic capacity of SM with a zero-forcing (ZF) receiver in transmit correlated Rayleigh MIMO channels was derived in [6]. Comparing this bound with the OSTBC capacity bound in (12) we find that there exists a crossing point of the capacity curves at an SNR threshold γ_{CP}, which corresponds to the positive solution to the polynomial

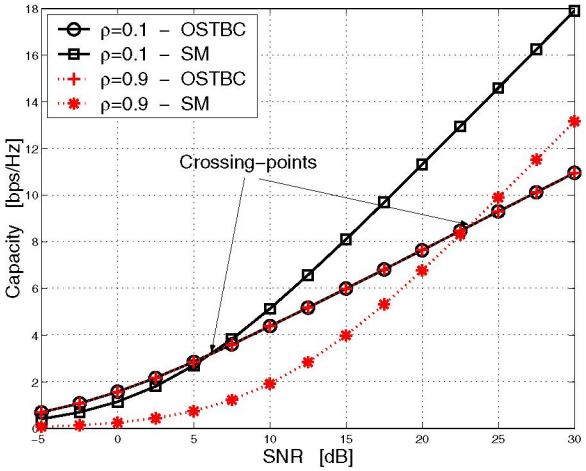

Fig. 2. Capacity crossing-points of OSTBC and SM for MIMO 2x2 systems, as a function of the transmit spatial correlation. The channel is single-sided correlated and the exponential model is used, with $\rho_{\text{tx}} = 0.1$ and $\rho_{\text{tx}} = 0.9$.

equation

$$\sum_{k=1}^{N_t} \gamma_{\text{CP}}^k \left(\frac{N_r - N_t + 1}{N_t} |\mathbf{S}| \right)^k \text{tr}_k(\mathbf{A}) + 1 = \left(\gamma \frac{N_r}{R_c} + 1 \right)^{R_c} \tag{13}$$

where $\mathbf{A} = \text{diag}\left(1/|\mathbf{S}^{11}|, \ldots, 1/|\mathbf{S}^{N_t N_t}|\right)$, $\text{tr}_k(\cdot)$ denotes the k^{th} elementary symmetric function and $\mathbf{S}^{kk}$ corresponds to $\mathbf{S}$ with the k^{th} row and column removed.

To gain further insight, we consider the special case of $N_t = 2$ and $N_r = 2$. By definition $\text{tr}_1(\mathbf{A}) = 2$ and $\text{tr}_2(\mathbf{A}) = 1$, and it is easily shown that the solution to (13) is given by

$$\gamma_{\text{CP}} = \frac{4}{|\mathbf{S}|} \left(\frac{2}{|\mathbf{S}|} - 1 \right) \tag{14}$$

where we assumed $R_c = 1$ for the Alamouti code. Noting that $|\mathbf{S}|$ is a decreasing function of the channel correlation, we see that γ_{CP}, defining the relative performance of OSTBC and SM, varies monotonically with the correlation, indicating that OSTBC is more resilient to correlation than SM.

Fig. 2 shows OSTBC capacity curves based on (12), and the SM-ZF capacity (derived in [6]), in low and high correlation scenarios. As expected, we see a crossing point between the respective OSTBC and SM curves, which moves significantly to the right (i.e. by approximately 16 dB) as the spatial correlation increases. This result suggests that practical adaptive switching strategies (such as the method proposed in Section V) should be designed to take into account not only the average SNR, but also the spatial correlation information.

IV. Error Probability of OSTBC with BICM in Double-Sided Correlated Channels

The results above show that significant information theoretic gains could be achieved by switching between OSTBC and SM, depending on the channel quality (measured by the SNR and spatial correlation). In practical systems however, sub-optimal low-complexity transmission strategies are typically employed, such as BICM. For these practical systems, the average BER is the performance measure of interest.

In this section we derive the BER of OSTBC with BICM in spatially-correlated channels. Note that the performance of OSTBC with BICM has been previously considered for *uncorrelated* channels in [13–15]. Our results are derived under the common assumption of ideal interleaving. These analytical results, along with corresponding BER expressions we derived previously for SM systems in [7], will form the basis of our practical adaptive switching algorithm proposed in Section V.

We consider a MIMO system operating with standard BICM encoders on each transmit layer with 2^M-ary Gray-labeled PSK/QAM modulation (e.g. see [16]). The modulated symbols output from the BICM encoder are then further formatted via an OSTBC encoder, prior to transmission across the channel.

From (4), clearly the k^{th} element of $\mathbf{z} \in \mathbb{C}^{n_s \times 1}$ corresponds to the output from a fading AWGN scalar channel, where the input is the k^{th} element of $\mathbf{a}$. For the k^{th} modulated symbol, a_k, the BICM log-likelihood metrics are then calculated for the corresponding bits i (= $1, \ldots, M$) according to [16]

$$\mathcal{L}_{k,i} = \ln \frac{\sum_{\tilde{a} \in \mathcal{A}_1^i} p\left(z_k | \tilde{a}, \mathbf{H}\right)}{\sum_{\tilde{a} \in \mathcal{A}_0^i} p\left(z_k | \tilde{a}, \mathbf{H}\right)} \tag{15}$$

where $\mathcal{A}_0^i$ and $\mathcal{A}_1^i$ denote the subsets of the (scalar) transmit constellation $\mathcal{A}$ with i^{th} bit equal to 0 and 1 respectively, z_k is the k^{th} element of $\mathbf{z}$, and

$$p\left(z_k | \tilde{a}, \mathbf{H}\right) = \frac{1}{\pi \|\mathbf{H}\|_F^2} \exp\left(- \frac{|z_k - \sqrt{\gamma} \|\mathbf{H}\|_F^2 \, \tilde{a}|^2}{\|\mathbf{H}\|_F^2} \right). \tag{16}$$

These metrics are deinterleaved, and decoded using a soft-decision Viterbi algorithm.

A. Saddlepoint Approximation for the Codeword Pairwise Error Probability (C-PEP)

The union bound on BER for BICM can be found directly from the C-PEP, $f(d, \mu, \mathcal{A}, \gamma)$, where d is the codeword Hamming distance and μ is the labeling map. For the case we are considering of BICM with OSTBC, we employ the analysis approach in [7, 8] based on the saddlepoint approximation [17, App. 5A]

$$f(d, \mu, \mathcal{A}, \gamma) \approx \frac{1}{\sqrt{2\pi d \mathcal{K}_{\mathcal{L}}''(\hat{s}) \hat{s}}} \mathcal{M}_{\mathcal{L}}(\hat{s})^d \tag{17}$$

where $\mathcal{M}_{\mathcal{L}}$ is the moment generating function (m.g.f.) of the likelihood ratio $\mathcal{L}$ at an arbitrary point in time, given by[3]

$$\mathcal{M}_{\mathcal{L}}(s) \triangleq E_{\mathcal{L}}\left[\exp(s\mathcal{L})\right] \tag{18}$$

and $\mathcal{K}_{\mathcal{L}}''(\hat{s})$ denotes the second derivative of the cumulant generating function $\mathcal{K}_{\mathcal{L}}(s) = \ln \mathcal{M}_{\mathcal{L}}(s)$, evaluated at the *saddlepoint* $\hat{s}$, which is the real minimizing value of $\mathcal{M}_{\mathcal{L}}(s)$.

For OSTBC transmission, the m.g.f. is easily obtained using (15), (16), and (18) as

$$\mathcal{M}_{\mathcal{L}}(s) = E_{\mathcal{V}}\left[\left(\frac{\sum_{\tilde{a} \in \mathcal{A}_u^m} \exp\left(- \frac{|\sqrt{\gamma}\|\mathbf{H}\|_F^2 (a_k - \tilde{a}) + \underline{n}_k|^2}{\|\mathbf{H}\|_F^2} \right)}{\sum_{\tilde{a} \in \mathcal{A}_u^m} \exp\left(- \frac{|\sqrt{\gamma}\|\mathbf{H}\|_F^2 (a_k - \tilde{a}) + \underline{n}_k|^2}{\|\mathbf{H}\|_F^2} \right)} \right)^s \right]$$

where, for notational convenience, we have grouped the expectation variables into the vector $\mathcal{V} = (a_k, m, u, k, \mathbf{H}, \underline{n}_k)$, where u is a uniform binary random variable.

[3]Note that, due to the time independence, we drop the $\mathcal{L}$ subscripts.

$$f(d,\mu,\mathcal{A},\gamma) \approx \frac{1}{2\sqrt{\pi d}} \frac{\left[\sum_{i=1}^{|\mathcal{P}_M|} \mathcal{P}_{M,i} \sum_{\ell=1}^{r} \left(1+\frac{\gamma \mathcal{E}_{M,i}\lambda_{q,\ell}}{4}\right)^{-1} \prod_{j=1,j\neq\ell}^{r} \left(\frac{\lambda_{q,\ell}}{\lambda_{q,\ell}-\lambda_{q,j}}\right)\right]^{d+\frac{1}{2}}}{\sqrt{\sum_{i=1}^{|\mathcal{P}_M|} \mathcal{P}_{M,i} \sum_{\ell=1}^{r} \left(1+\frac{\gamma \mathcal{E}_{M,i}\lambda_{q,\ell}}{4}\right)^{-2} \left(\frac{\gamma \mathcal{E}_{M,i}\lambda_{q,\ell}}{4}\right) \prod_{j=1,j\neq\ell}^{r} \left(\frac{\lambda_{q,\ell}}{\lambda_{q,\ell}-\lambda_{q,j}}\right)}} \tag{22}$$

$$f(d,\mu,\mathcal{A},\gamma) \approx \frac{1}{2\sqrt{\pi d}} \left[\sum_{i=1}^{|\mathcal{P}_M|} \mathcal{P}_{M,i} \sum_{\ell=1}^{r} \left(1+\frac{\gamma \mathcal{E}_{M,i}\lambda_{q,\ell}}{4}\right)^{-1} \prod_{j=1,j\neq\ell}^{r} \left(\frac{\lambda_{q,\ell}}{\lambda_{q,\ell}-\lambda_{q,j}}\right)\right]^{d} \tag{24}$$

In general, this equation does not admit a closed-form solution. At high SNR, however, closed-form solutions do exist and these provide an approximation for all SNRs. Following the general approach in [7, 8] we average over the uniform bit-positions m, bit-swapping values u, and symbols $a_k \in \mathcal{A}_u^m$, and apply the Dominated Convergence Theorem to obtain

$$\mathcal{M}_{\mathcal{L}}(s) = \sum_{i=1}^{|P_M|} \mathcal{P}_{M,i}\, \mathcal{I}_{\mathcal{E}_{M,i}}(s) \tag{19}$$

where the sets $\mathcal{P}_M$ (with cardinality $|\mathcal{P}_M|$) and $\mathcal{E}_M$ are defined in Table I, with i^{th} element $\mathcal{P}_{M,i}$ and $\mathcal{E}_{M,i}$ respectively, and

$$\mathcal{I}_{\mathcal{E}_{M,i}}(s) = E_{\underline{n},\mathbf{H}}\left[\left(\frac{\exp\left(-\frac{|\sqrt{\gamma}\|\mathbf{H}\|_F^2\sqrt{\mathcal{E}_{M,i}}+\underline{n}|^2}{\|\mathbf{H}\|_F^2}\right)}{\exp\left(-\frac{|\underline{n}|^2}{\|\mathbf{H}\|_F^2}\right)}\right)^{s}\right]$$

where $\underline{n} \sim \mathcal{CN}(0, \|\mathbf{H}\|_F^2)$. Averaging over $\underline{n}$, and using (6) gives

$$\mathcal{I}_{\mathcal{E}_{M,i}}(s) = E_{\eta}\left[\exp\left(-\frac{\gamma\,\eta\,\mathcal{E}_{M,i}s(1-s)}{2}\right)\right]. \tag{20}$$

Finally, we use (8) to obtain

$$\mathcal{I}_{\mathcal{E}_{M,i}}(s) = \sum_{\ell=1}^{r} \prod_{j=1,j\neq\ell}^{r} \left(\frac{\lambda_{q,\ell}}{\lambda_{q,\ell}-\lambda_{q,j}}\right) \frac{1}{(1+\mathcal{E}_{M,i}\lambda_{q,\ell}s(1-s))}. \tag{21}$$

Noting that the m.g.f. (19) is minimized at the saddlepoint $\hat{s} = \frac{1}{2}$, and using (21) and (19) in (17), we obtain the saddlepoint approximation to the C-PEP given by (22).

B. Simplified C-PEP

Applying the following approximation to the denominator of (22)

$$\left(\frac{\gamma \mathcal{E}_{M,i}\lambda_{q,\ell}}{4}\right) \approx \left(\frac{\gamma \mathcal{E}_{M,i}\lambda_{q,\ell}}{4}\right) + 1 \tag{23}$$

we obtain a simplified C-PEP expression given by (24).

C. Performance Results

Fig. 3 compares the preceding analytical BICM-OSTBC BER expressions with Monte-Carlo simulation results, for a 2×2 system with various Gray-labeled constellations. Results are presented for the optimal 64-state 1/2 rate binary convolutional code with $d_{\text{free}} = 10$. The 'saddlepoint' curves were obtained from the C-PEP expression (22), and are clearly tight for low to moderate BERs. The 'saddlepoint (approx)' curves were obtained from (24), and are within 1 dB of the simulated curves in all cases.

	$\mathcal{P}_M$	$\mathcal{E}_M$
BPSK	{1}	{4.0}
QPSK	{1}	{2.0}
16QAM	{3/4, 1/4}	{0.4, 1.6}
64QAM	{7/12, 1/4, 1/12, 1/12}	{ 0.0952, 0.3810, 0.8571, 1.5238}

TABLE I

BREAKDOWN OF DISTANCE MULTIPLICITIES BETWEEN COMPLEMENT BICM SUBSETS FOR VARIOUS CONSTELLATIONS WITH GRAY LABELING

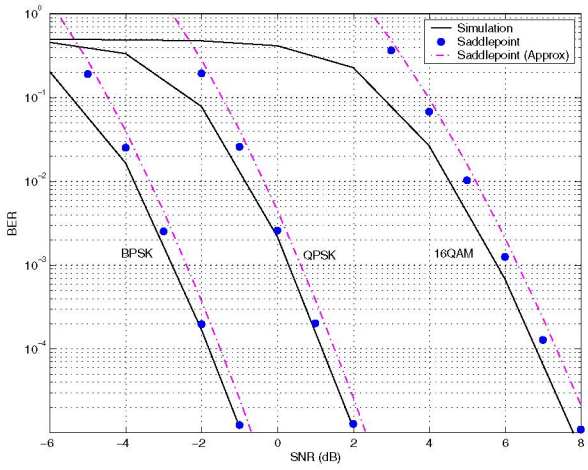

Fig. 3. Simulated and analytical BER of 2×2 BICM-OSTBC employing the optimal $\frac{1}{2}$ rate code ($d_{\text{free}} = 10$). The exponential model is used, with $\rho_{\text{tx}} = 0.5$ and $\rho_{\text{rx}} = 0.1$.

V. Practical Adaptive MIMO Algorithm

We now propose an adaptive MIMO transmission algorithm based on theoretical BER expressions we have just derived. The algorithm switches between BICM-OSTBC and BICM-SM and exploits the statistical channel information (i.e., average SNR and channel spatial correlation). To enable transmission over the wireless link we define a set of transmission *modes*, which are combinations of modulation/coding schemes (MCSs) and MIMO transmission techniques (i.e., OSTBC or SM). We use the eight MCSs proposed in the IEEE 802.11a standard for wireless local area networks, with increasing values of data rate (R). The key idea of the algorithm is to compute the theoretical BER for given channel condition and

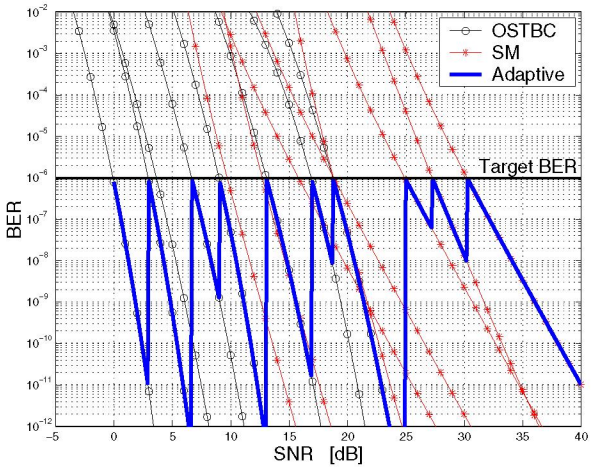

Fig. 4. BER performance for adaptive MIMO 2x2 systems. The BER of OSTBC and SM are obtained from the approximations in (24) and [7], respectively. The exponential model is used, with $\rho_{\text{tx}} = 0.1$ and $\rho_{\text{rx}} = 0.05$.

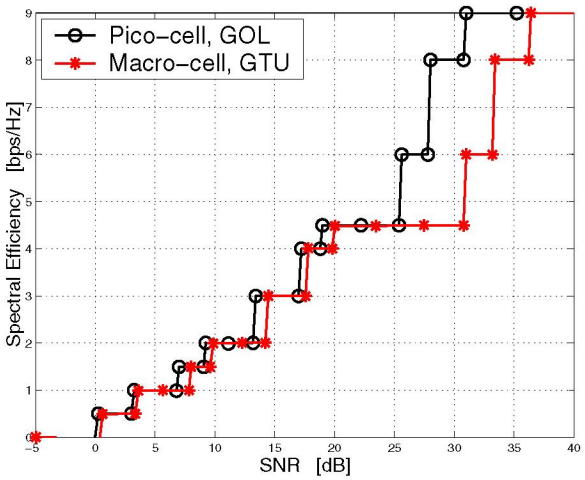

Fig. 5. Spectral efficiency for adaptive MIMO 2x2 systems in different propagation scenarios. The MIMO channel is simulated according to the COST-259 physical channel model [9]. Two channel environments are considered: "Pico-cell, GOL" and "Macro-cell, GTU".

select the transmission mode that yields the highest spectral efficiency while satisfying a predefined target BER.

Fig. 4 depicts the theoretical BER performance of different modes in double-sided spatially correlated channels, with $\rho_{\text{tx}} = 0.1$ and $\rho_{\text{rx}} = 0.05$. The curves with circles represent the BER for the eight MCSs with BICM-OSTBC derived from (24), and the curves with stars refer to the closed-form BER expression of BICM-SM in [7]. The performance of the adaptive algorithm with predefined target BER of 10^{-6} is depicted with the solid curve. It is possible to see that, for given transmit/receive spatial correlation, as the SNR increases the proposed adaptive method switches to the higher order modes to enhance the spectral efficiency while satisfying the predefined target BER. Note that in Fig. 4 we applied the adaptive algorithm to the theoretical BER in (24) and [7], rather than empirical BER derived from simulations. In practical systems, the switching thresholds can be empirically adjusted to compensate for the small SNR gap between theoretical and simulated BER curves shown in Fig. 3.

Next, we show the performance of the proposed method in terms of spectral efficiency, $R(1 - \text{BER})$, for the same target BER of 10^{-6}. We simulated the propagation channel according to the COST-259 physical channel model [9] and assumed uniform linear array (ULA) configuration with half-wavelength element spacing both at the transmitter and receiver. Two different radio environments are simulated: pico-cell with generalized office line-of-sight (GOL) defined with 8 clusters and random generated AS and AOA/AOD; macro-cell with generalized typical urban (GTU) defined with single cluster, AS$= 10^{\circ}$ and angle of arrival/departure of $= 0^{\circ}$ (i.e., broadside directions). The transmit/receive spatial correlation matrices are computed by averaging the instantaneous MIMO channel over time. Fig. 5 shows that in high SNR regime our proposed adaptive MIMO algorithm doubles the spectral efficiency of conventional systems employing adaptive MCSs with fixed OSTBC transmission scheme. It is possible to see that the performance of the adaptive algorithm is better in "Pico-cell, GOL" due to the higher number of clusters that yield lower spatial correlation.

REFERENCES

[1] V. Tarokh, H. Jafarkhani, and A. R. Calderbank, "Space-time block codes from orthogonal designs," *IEEE Trans. Info. Th.*, vol. 45, pp. 1456–467, Jul. 1999.

[2] G. J. Foschini, G. D. Golden, R. A. Valenzuela, and P. W. Wolniansky, "Simplified processing for high spectral efficiency wireless communication employing multi-element arrays," *IEEE Jour. Select. Areas in Comm.*, vol. 17, no. 11, pp. 1841 – 1852, Nov. 1999.

[3] L. Zheng and D. N. C. Tse, "Diversity and multiplexing: a fundamental tradeoff in multiple-antenna channels," *IEEE Trans. Info. Th.*, vol. 49, no. 5, pp. 1073–1096, May 2003.

[4] R. W. Heath and A. J. Paulraj, "Switching between diversity and multiplexing in MIMO systems," *IEEE Trans. Comm.*, vol. 53, no. 6, pp. 962 – 968, Jun. 2005.

[5] S. Catreux, V. Erceg, D. Gesbert, and R. W. Heath Jr., "Adaptive modulation and MIMO coding for broadband wireless data networks," *IEEE Comm. Mag.*, vol. 2, pp. 108–115, June 2002.

[6] A. Forenza, M. R. McKay, A. Pandharipande, R. W. Heath Jr., and I. B. Collings, "Capacity enhancement via multi-mode adaptation in spatially correlated MIMO channels," in *IEEE Int. Conf. on Pers., Indoor, Mobile, and Radio Comm. (PIMRC)*, Berlin, Germany, Sep 2005.

[7] M. R. McKay, I. B. Collings, A. Forenza, and R. W. Heath Jr., "A throughput-based adaptive MIMO-BICM approach for spatially-correlated channels," *to appear in Proc. IEEE ICC*, June 2006.

[8] A. Martinez, A. G. Fàbregas, and G. Caire, "New simple evaluation of the error probability of bit-interleaved coded modulation using the saddlepoint approximation," in *Proc. IEEE Int. Symp. on Info. Theory and Appl. (ISITA)*, Oct. 2004.

[9] L. M. Correia, *Wireless Flexible Personalised Communications*, John Wiley and Sons, Inc., New York, NY, USA, 2001.

[10] B. Hassibi and B. M. Hochwald, "High-rate codes that are linear in space and time," *IEEE Trans. Info. Th.*, vol. 48, pp. 1804–1824, July 2002.

[11] A. M. Mathai and S. B. Provost, *Quadratic Forms in Random Variables*, Marcell Dekker, Inc., New York, NY, 1992.

[12] I. S. Gradshteyn and I. M. Ryzhik, *Table of Integrals, Series, and Products*, Academic Press Inc., New York, NY, 1st edition, 1994.

[13] Z. Hong and B. L. Hughes, "Robust space-time codes for time-selective fading," in *IEEE Info. The. Wkshop*, Australia, 2001, pp. 112–114.

[14] M. R. McKay and I. B. Collings, "Throughput performance of low complexity MIMO extensions to OFDM-based WLANs," in *IEEE Int. Symp. on Spread Spec. Tech. and Applic.*, Sydney, Australia, Aug. 2004.

[15] E. Akay and E. Ayanoglu, "Bit interleaved coded modulation with space time block codes for OFDM systems," in *IEEE Vehicular Technology Conference*, Los Angeles, USA, 2004, pp. 2477–2481.

[16] M. R. McKay and I. B. Collings, "Capacity and performance of MIMO-BICM with zero forcing receivers," *IEEE Trans. Commun.*, vol. 53, no. 1, pp. 74–83, Jan. 2005.

[17] R. Gallagher, *Information Theory and Reliable Communication*, John Wiley and Sons, 1968.